ELSEVIER

Journal of Chromatography A, 760 (1997) 41–53

JOURNAL OF CHROMATOGRAPHY A

Prediction of the preparative chromatography performance with a very small column

Oliver Kaltenbrunner[a], Alois Jungbauer[a,*], Shuichi Yamamoto[b]

[a]*Institute of Applied Microbiology, University of Agriculture, Forestry and Biotechnology, Nussdorferlände 11, A-1190 Vienna, Austria*
[b]*Department of Chemical Engineering, Yamaguchi University, Tokiwadai, Ube 755, Japan*

Abstract

Practical considerations lead to the use of small columns in preparative chromatography. In these applications extra column effects may overwhelm all broadening effects. The influence of the extra column effects on the band broadening and migration is demonstrated by simulation. The model assumes linearity of extra column effects. Consequently, these effects could be described by the convolution of the initial applied band width, an exponential decay and Gaussian broadening. An attempt has been made to discriminate between the column, pre- and postcolumn broadening.

Keywords: Preparative chromatography; Extra-column effects; Simulation; Band broadening; Peak shape

1. Introduction

A small column in preparative chromatography is defined by the ratio between extra column space and column volume. Considering conventional laboratory equipment for bench scale chromatography, such as BioCAD (Perseptive Biosystems, Cambridge, MA, USA), ProSys (BioSepra, Marlborough, MA, USA), FPLC, BioPilot and Ekta (all Pharmacia Biotech, Uppsala, Sweden), the volume of a small column is in the order of less than a few ml. For several applications these small columns are required. Determination of adsorption isotherms by chromatographic means or validation of clearance of adventitious agents should be carried out at a very small scale. Often process development is restricted by a shortage of starting material since pilot production and pilot purification are developed simultaneously. A very small column can circumvent this obstacle.

The benefits of small scale are reduced time for experiments and the requirement of only small amounts of materials and buffers. These benefits may be overcome by a more difficult interpretation of the results due to dominating extra column effects. In the past, scale down of preparative chromatography has not been frequently investigated. Studies of extra column band broadening were reported by Sternberg [1], Huber and Rizzi [2] and Dose and Guiochon [3]. Sternbergs considerations were derived for gas chromatography. Nevertheless, most of them are applicable to liquid chromatography [4] under the restriction of the hydrodynamic differences of gases and liquids. Rocca et al. [5] described the band broadening of different column configurations without special emphasizing on extra column influence. Models for prediction of peak profiles normally neglect the extra column influence [6–9].

An attempt has been made to predict extra column peak broadening for very small columns. Experiments with different size at identical extra column space (identical tubing, valves, adapters, safety devices, etc.) allow an accurate determination of the

*Corresponding author

PII S0021-9673(96)00689-9

extra column band spreading. Assuming the contributions of the extra column band spreading independent of the applied sample volume, an exponential modified Gaussian function has been developed in order to circumvent the commonly applied assumption of a sample shape such as a Dirac delta function. The influence of the band spreading before and after the column is described by a function derived by convoluting a rectangular pulse, an exponential decay and a Gaussian contribution to broadening in the Laplace domain. Once the parameters of the system are acquired, the extra column profile of any sample volume can be predicted. An attempt has been made to discriminate between the pre and post column effects. This model has been connected to a computer simulation for migration and band spreading in the column [10]. This simulation program is based on a discontinuous stage model. By applying this simulation, the influence of the extra column effects and the column effects (nonlinearity of isotherm, axial dispersion) on the total band broadening can be demonstrated. These models are considered as a contribution to scale up, scale down and computer assisted optimization of chromatography.

2. Theory

In order to describe the behavior of a protein sample in different scales of chromatographic systems, the influence of the extra column space on the band broadening must be distinguished from the broadening occurring in the column. A comprehensive description of the extra column effects on gas chromatography is given by Sternberg [1]. Most of the explanations are also valid for liquid chromatography [4].

The extra column effects can be subdivided into dispersion in tubes, contributions of dead volumes, finite detector volume and dynamic behavior of transducers and electronics.

According to Taylor [11], tubes introduce a symmetrical Gaussian-type broadening (σ_t^2) to the sample. The band spreads under the combined action of molecular diffusion and the parabolic axial flow velocity profile. For a fully developed laminar flow profile, this broadening can be described by

$$\sigma_t^2 = \frac{t_R \cdot r^2}{24 \cdot D_M} \tag{1}$$

where t_R is the retention time, r the radius of the tube and D_M the molecular diffusion coefficient.

Dead volumes create a type of wash out kinetic [12]. Therefore they introduce an exponential contribution to the band broadening. This exponential contribution (τ_{dead}) is a function of the dead volume (V_{dead}) and the flow-rate (F)

$$\tau_{dead} = \frac{V_{dead}}{F} \tag{2}$$

It was also shown by Sternberg [1] that the finite sensing volume of a detector introduces an additional symmetrical, rectangular broadening. This broadening (σ_d) depends on the sensitive detector volume (V_d) and the flow-rate. According to Cram and Glenn [12] it can be described by

$$\sigma_d^2 = \frac{V_d^2}{12 \cdot F^2} \tag{3}$$

An exponential contribution to the band broadening is introduced by the finite response rate of the electronically amplifier and recorder. This contribution (τ_{el}) is independent on the flow-rate [12,13].

Assuming additivity of the variances the total extra column broadening can be written as

$$\sigma_{ex}^2 = \sigma_s^2 + \sigma_t^2 + \sigma_d^2 + \tau_{dead}^2 + \tau_{el}^2 \tag{4}$$

where σ_{ex}^2 is the lumped extra column dispersion and σ_s^2 is the variance of the initial theoretical injection profile. Assuming in liquid chromatography the variances introduced by the electronics and the detector volume are negligible small compared to the other variances, Eq. (1) simplifies to

$$\sigma_{ex}^2 = \sigma_s^2 + \sigma_t^2 + \tau_{dead}^2 \tag{5}$$

Lumping together the variances independent of flow-rate (σ_A^2) and the variances dependent on flow-rate (σ_B^2) the extra column broadening σ_{ex}^2 is

$$\sigma_{ex}^2 = \sigma_A^2 + \frac{\sigma_B^2}{F^2} \tag{6}$$

An equation for the prediction of the extra column contribution to the total broadening can be derived

based on the definition of the plate number N of a system

$$N = \frac{V_R^2}{\sigma_{c.i.}^2} \tag{7}$$

If the total broadening (σ_{total}^2) is considered as the sum of the column internal broadening ($\sigma_{c.i.}^2$) and the extra column broadening (σ_{ex}^2)

$$\sigma_{total}^2 = \sigma_{c.i.}^2 + \sigma_{ex}^2 \tag{8}$$

the following relationship can be obtained

$$\sigma_{total}^2 = \frac{1}{N} \cdot V_R^2 + \sigma_{ex}^2 = \frac{HETP}{L} \cdot V_R^2 + \sigma_{ex}^2 \tag{9}$$

This equation has been derived for analytical chromatography by Huber and Rizzi [2].

Using this relationship it is possible to exhibit a quantitative picture of the contribution of extra column broadening on the total broadening.

For a peak prediction program using non-linear adsorption isotherms, the initial loading profile, in particular the loading concentration, is of crucial importance. The theoretically rectangular sample plug is altered by extra column effects and if the sample volume does not exceed a certain limit, the sample concentration arriving at the top of the column (C^*) is lower than concentration initially applied to the system (C_0). To allow a flexible description of these extra column alterations of a sample band an extended exponentially modified Gaussian model is applied. The normal exponentially modified Gaussian model [14] assumes an infinitely small sample band, what is a valid assumption for analytical chromatography. In the case of discrepancies from this assumption, the additional broadening of the sample pulse is lumped to the Gaussian parameter σ. To describe the different shapes of loading profiles dependent on the loading volume and the broadening introduced by the experimental setup we derived a function dependent on the loading volume and symmetrical and asymmetrical contributions to band broadening. Therefore, the convolution theorem of Laplace transforms was applied. The Laplace transforms of a rectangular plug, representing the theoretical loading profile, was convoluted with and exponential decay function, representing the influence of the dead volumes. The resulting convolution was inverted and used as an input function for the convolution integral technique according to Sternberg [1]. The following is a detailed description of this approach:

According to Jönsson [4] the Laplace transform of a rectangular plug

$$C(t) = \begin{cases} 0, & \text{if } t < 0 \\ C_0, & \text{if } 0 \le t \le \tau_r \\ 0, & \text{if } t > \tau_r \end{cases}$$

can be described as

$$L[f](s) = \frac{1 - e^{-s\tau_r}}{s} \tag{10}$$

and the Laplace transform of a normalized exponential decay

$$f(t) = \begin{cases} 0, & \text{if } t < 0 \\ \dfrac{e^{-\frac{t}{\tau_e}}}{\tau_e} & \text{if } t \ge 0 \end{cases}$$

can be described as

$$L[h](s) = \frac{1}{s \cdot \tau_e + 1} \tag{11}$$

Convolution of Eqs. (10) and (11) gives

$$L[f \cdot h](s) = \frac{\tau_e \cdot e^{-s \cdot \tau_r}}{s \cdot \tau_e + 1} - \frac{e^{-s \cdot \tau_r}}{s} - \frac{\tau_e}{s \cdot \tau_e + 1} + \frac{1}{s} \tag{12}$$

and the inversion to the time domain is

$$f(t) = L^{-1}[f \cdot h](s)$$
$$= \Lambda(t - \tau_r) \cdot \left(e^{-\frac{t-\tau_r}{\tau_e}} - 1 \right) - e^{-\frac{t}{\tau_e}} + 1 \tag{13}$$

where $\Lambda(t < \tau_r)$ is a unit step function with

$f(t) = 0$ for $t < \tau_r$ and $f(t) = 1$ for $t > \tau_r$

Using this function as an input function $f(t_a)$ for a convolution integral

$$g(t) = \frac{1}{\sqrt{2\pi} \cdot \sigma} \cdot \int_{t_{a_{min}}}^{t_{a_{max}}} f(t_a) \cdot e^{-\frac{(t - t_a)^2}{2\sigma^2}} dt_a \tag{14}$$

we get

$$g(t) = \frac{1}{\sqrt{2\pi}\cdot\sigma} \cdot \int_{t_R}^{\infty} \left[A(t_a - t_R - \tau_r) \cdot \left(e^{-\frac{t_a - t_R - \tau_r}{\tau_e}} - 1 \right) - e^{-\frac{t_a - t_R}{\tau_e}} + 1 \right] \cdot e^{-\frac{(t-t_a)^2}{2\sigma^2}} dt_a \quad (15)$$

assuming $\sigma > 0$ and $\tau_r > 0$ the integration of Eq. (15) gives

$$g(t) = T_6 \cdot \left\{ \frac{T_5 \cdot [\mathrm{erf}(T_1 - T_4 - T_3) + 1]}{2} - \frac{\mathrm{erf}(T_1 - T_4 - T_2) + 1}{2} \right\} - \frac{\mathrm{erf}(T_1 - T_3) - \mathrm{erf}(T_1 - T_2)}{2} \quad (16)$$

with

$$T_1 = \frac{\sqrt{2}\cdot t}{2\sigma} \quad (17)$$

$$T_2 = \frac{\sqrt{2}\cdot t_R}{2\sigma} \quad (18)$$

$$T_3 = \frac{\sqrt{2}\cdot (t_R + \tau_r)}{2\sigma} \quad (19)$$

$$T_4 = \frac{\sqrt{2}\cdot \sigma}{2\tau_e} \quad (20)$$

$$T_5 = e^{\frac{\tau_r}{\tau_e}} \quad (21)$$

$$T_6 = e^{\frac{\sigma^2}{2\cdot\tau_e^2} - \frac{t - t_R}{\tau_e}} \quad (22)$$

In these functions t_R denotes for the retention time, σ for the Gaussian broadening, τ_e for the exponential decay and τ_r for the with of the initial sample plug.

For adsorption chromatography it is a poor simplification to describe all extra column effects with one function altering the loading profile of a column. As the protein sample is caught at a small zone of the column it is sharpened and concentrated. The extra column effects prior to the column are overwhelmed by the column effects. On the other hand, the broadening in the column effluent can effect the experimental peaks while the predicted peaks are not altered post column in any way. Unfortunately, it seems to be impossible to get experimental data to distinguish between pre and post column extra column broadening. As a result, only estimations of ratios between pre- and post column broadening can be combined to the predicted profiles. To get an insight of the possibilities to split the loading function Eq. (16) into a pre and a post column component, different ratios of pre and post column broadenings were combined. The broadening was combined assuming additivity of the Gaussian variances:

$$\sigma^2_{\mathrm{total}} = \sum_{i=1}^{n} \sigma_i^2 \quad (23)$$

Thus, if the total extra column ($\sigma^2_{\mathrm{total}}$) broadening is divided into a pre (σ^2_{pre}) and a post column part (σ^2_{post}) Eq. (24) can be written as

$$\sigma^2_{\mathrm{total}} = \sigma^2_{\mathrm{pre}} + \sigma^2_{\mathrm{post}} \quad (24)$$

For a defined ratio x between pre and post column broadening the Gaussian broadenings can be calculated as

$$\sigma^2_{\mathrm{pre}} = x \cdot \sigma^2_{\mathrm{total}}$$
$$\sigma^2_{\mathrm{post}} = (1 - x) \cdot \sigma^2_{\mathrm{total}} \quad (25)$$

Unfortunately, exponential decays are not additive. Naor and Shinnar [15] gave insights of properties of some theoretical residence time distributions including non-identical mixing vessels in series. Since it is not possible to determine the pre and post column contribution to broadening experimentally, a more theoretical approach is applied. Analogous to the procedure given in Eqs. (10–16) to a convolution of a plug input profile with two non-identical exponential decays and a Gaussian broadening was carried out.

The convolution of Eqs.

$$L[f](s) = \frac{1 - e^{-s\cdot\tau_r}}{s},$$

$$L[h_1](s) = \frac{1}{s\cdot\tau_{e_1} + 1} \quad \text{and}$$

$$L[h_2](s) = \frac{1}{s\cdot\tau_{e_2} + 1}$$

gives

$$L[f\cdot h_1\cdot h_2](s)$$
$$=\frac{\tau_{e_2}^2\cdot\exp(-s\cdot\tau_r)}{(s\cdot\tau_{e_1}+1)\cdot(\tau_{e_1}-\tau_{e_2})}+\frac{\tau_{e_1}\cdot\exp(-s\cdot\tau_r)}{s\cdot\tau_{e_1}+1}$$
$$+\frac{\tau_{e_2}\cdot\exp(-s\cdot\tau_r)}{s\cdot\tau_{e_1}+1}-\frac{\tau_{e_2}^2\cdot\exp(-s\cdot\tau_r)}{(s\cdot\tau_{e_2}+1)\cdot(\tau_{e_1}-\tau_{e_2})}$$
$$-\frac{\exp(-s\cdot\tau_r)}{s}-\frac{\tau_{e_2}}{(s\cdot\tau_{e_1}+1)\cdot(\tau_{e_1}-\tau_{e_2})}$$
$$-\frac{\tau_{e_1}}{s\cdot\tau_{e_1}+1}-\frac{\tau_{e_2}}{s\cdot\tau_{e_2}+1}$$
$$+\frac{\tau_{e_2}^2}{(s\cdot\tau_{e_2}+1)\cdot(\tau_{e_1}-\tau_{e_2})}+\frac{1}{s} \quad (26)$$

The inversion of the Laplace transform into the time domain gives

$$f(t)=L^{-1}[f\cdot h_1\cdot h_2](s)$$
$$=\Lambda(t-\tau_r)\cdot\frac{\tau_{e_2}^2}{\tau_{e_1}\cdot(\tau_{e_1}-\tau_{e_2})}\cdot\exp\left(-\frac{t-\tau_r}{\tau_{e_1}}\right)$$
$$+\Lambda(t-\tau_r)\cdot\exp\left(-\frac{t-\tau_r}{\tau_{e_1}}\right)+\Lambda(t-\tau_r)\cdot\frac{\tau_{e_2}}{\tau_{e_1}}$$
$$\cdot\exp\left(-\frac{t-\tau_r}{\tau_{e_1}}\right)-\Lambda(t-\tau_r)\cdot\frac{\tau_{e_2}}{(\tau_{e_1}-\tau_{e_2})}$$
$$\cdot\exp\left(-\frac{t-\tau_r}{\tau_{e_1}}\right)-\Lambda(t-\tau_r)-\frac{\tau_{e_2}^2}{\tau_{e_1}\cdot(\tau_{e_1}-\tau_{e_2})}$$
$$\cdot\exp\left(-\frac{t}{\tau_{e_1}}\right)-\exp\left(-\frac{t}{\tau_{e_1}}\right)-\frac{\tau_{e_2}}{\tau_{e_1}}$$
$$\cdot\exp\left(-\frac{t}{\tau_{e_1}}\right)+\frac{\tau_{e_2}}{(\tau_{e_1}-\tau_{e_2})}\cdot\exp\left(-\frac{t}{\tau_{e_1}}\right)+1 \quad (27)$$

where $\Lambda(t<\tau_r)$ is a unit step function with $f(t)=0$ for $t<\tau_r$ and $f(t)=1$ for $t>\tau_r$. Using equation as an input function for the convolution integral Eq. (24) and assuming $\tau_r>0$ and $\sigma>0$ leads to

$$g(t)=\frac{1}{2}(-T_1\cdot T_2+T_3\cdot T_4-T_5+T_6\cdot T_2-T_7\cdot T_4+T_8) \quad (28)$$

with

$$T_1=\exp\left(\frac{\sigma^2}{2\cdot\tau_{e_1}^2}-\frac{t-t_R-\tau_r}{\tau_{e_1}}\right)\cdot\left[\operatorname{erf}\left(\frac{\sigma}{\sqrt{2}\cdot\tau_{e_1}}-\frac{t-t_R-\tau_r}{\sqrt{2}\cdot\sigma}\right)-1\right] \quad (29)$$

$$T_2=\frac{\tau_{e_2}^2}{\tau_{e_1}\cdot(\tau_{e_1}-\tau_{e_2})}+\frac{\tau_{e_2}}{\tau_{e_1}}+1 \quad (30)$$

$$T_3=\exp\left(\frac{\sigma^2}{2\cdot\tau_{e_2}^2}-\frac{t-t_R-\tau_r}{\tau_{e_2}}\right)\cdot\left[\operatorname{erf}\left(\frac{\sigma}{\sqrt{2}\cdot\tau_{e_2}}-\frac{t-t_R-\tau_r}{\sqrt{2}\cdot\sigma}\right)-1\right] \quad (31)$$

$$T_4=\frac{\tau_{e_2}}{\tau_{e_1}-\tau_{e_2}} \quad (32)$$

$$T_5=\left[\operatorname{erf}\left(\frac{t-t_R-\tau_r}{\sqrt{2}\cdot\sigma}\right)+1\right] \quad (33)$$

$$T_6=\exp\left(\frac{\sigma^2}{2\cdot\tau_{e_1}^2}-\frac{t-t_R}{\tau_{e_1}}\right)\cdot\left[\operatorname{erf}\left(\frac{\sigma}{\sqrt{2}\cdot\tau_{e_1}}-\frac{t-t_R}{\sqrt{2}\cdot\sigma}\right)-1\right] \quad (34)$$

$$T_7=\exp\left(\frac{\sigma^2}{2\cdot\tau_{e_2}^2}-\frac{t-t_R}{\tau_{e_2}}\right)\cdot\left[\operatorname{erf}\left(\frac{\sigma}{\sqrt{2}\cdot\tau_{e_2}}-\frac{t-t_R}{\sqrt{2}\cdot\sigma}\right)-1\right] \quad (35)$$

$$T_8=\left[\operatorname{erf}\left(\frac{t-t_R}{\sqrt{2}\cdot\sigma}\right)+1\right] \quad (36)$$

This approach can be used to fit the response peak and to get values for τ_{e_1} and τ_{e_2}. Then these parameters can be inserted into Eq. (17) for the pre column space and for the post column area.

3. Materials and methods

3.1. Chromatography system

Two chromatography systems were used. First, two high-performance pumps P-3500 (Pharmacia Biotech) were controlled by a liquid chromatography

controller LCC-500 plus (Pharmacia Biotech). The column effluent was monitored by a monitor UV-M (Pharmacia Biotech) at 280 nm and a conductivity monitor (Pharmacia Biotech). The analog signals were transferred to a PE Nelson 900 Series Interface and stored digitally by a Model 2600 chromatography software, Rev. 4.1 (Nelson Analytical, Cupertino, CA, USA). Samples were injected by a motor valve PMV-7 (Pharmacia Biotech), or in case of frontal analysis, the sample was loaded by a P-3500 pump.

Second, a ProSys chromatography system (BioSepra) was used. The pump module contains 4 single piston pumps delivering up to 30 ml/min each and mixing devices to allow buffer blending from up to 4 stock solutions. The separation module consists of two 6 port 2 position Rheodyne 9700 series polyether ether ketone (PEEK) switching valves, a Rheodyne 9700 series PEEK injection valve, a Beckman Model 166 variable wavelength detector for variable wavelengths from 190 to 700 nm with a flow cell of 1.1 μl and 2.5 mm path length, a pH monitor, a conductivity monitor and an A/D converter with software selectable data rates from 0.1 to 10 Hz. The whole system is controlled by a ProSys workstation installed on a 486/66 CPU with 8 Mbytes Ram.

3.2. Sorbent

Q-HyperD-F, an anion-exchanger was obtained by BioSepra.

3.3. Buffers

For all experiments, a 10 m*M* Tris–HCl buffer pH 8.0 added with 1 *M* NaCl was used.

3.4. Samples

As a model protein, highly purified bovine serum albumin (Sigma, St. Louis, MO, USA; Catalog No. A-6918) was used. The lyophilized powder was reconstituted in equilibration buffer and prepared freshly for each set of experiments.

3.5. Numerical treatment of data

Raw data from the chromatograms are exported from the Nelson data acquisition software as well as from the ProSys workstation to all other programs as tab-delimited textfiles. In isocratic and linear gradient experiments, these data were fitted with exponential modified Gaussian peaks [16]. Fitting was carried out by using the software Peak Fit version 3.18 (©1993) and version 4.0 (©1995, Jandel Scientific, San Rafael, CA, USA).

3.6. Approximation of error functions

For the calculation of these equations error functions are needed. According to Abromowitz and Stegun [17] an error function can be approximated using following procedure:

$$\begin{aligned} \mathrm{erf}(x) &= \mathrm{erf}(x) \quad \text{for } x > 0 \\ \mathrm{erf}(x) &= -\mathrm{erf}|x| \quad \text{for } x > 0 \end{aligned} \tag{37}$$

and

$$\mathrm{erf}(x) = 1 - (a_1 \cdot t + a_2 \cdot t^2 + a_3 \cdot t^3 + a_4 \cdot t^4 + a_5 \cdot t^5) \cdot e^{-x^2} \tag{38}$$

where

$$t = \frac{1}{1 + p \cdot x} \tag{39}$$

and $p = 0.3275911$, $a_1 = 0.254829592$, $a_2 = -0.284496736$, $a_3 = 1.42143741$, $a_4 = -1.453152027$, $a_5 = 1.061405429$. Using these equations the approximation error (ε) for $0 < x < \infty$ is $|\varepsilon| < 1.5 \cdot 10^{-7}$.

4. Results

To distinguish the contribution of extra column from the broadening occurring in the column, detailed analysis of extra column broadening and total broadening were carried out. The retention times and variances of protein pulses applied on columns under non-binding conditions with different heights of packed beds were used for these investigations. Extra column effects can be estimated by extrapolation of experimental data from different column sizes to an infinite small column volume.

A column with 5 mm I.D. was packed with the anion-exchanger Q-HyperD with 0.77, 2.2, 3.4, 5.3, 9.2 and 18.3 cm bed height. Additionally, the flow distributors of the column were connected without any resin. Using these different columns, pulse experiments were carried out at the flow-rates 0.1, 0.25, 0.5, 1.0 and 2.0 ml/min (30.6, 76.4, 152.8, 305.6 and 611.2 cm/h) in triplicates. For comparative reasons, the time axis was transformed to a volume axis.

Plotting the retention volumes (V_R) against the total column volume gives a hint on the reproducibility of the different packings (Fig. 1). The good agreement of the data points with a straight line indicate a high reproducibility in column packing. Additionally, the void fraction and the extra column volume can be calculated using this plot. The slope and the intercept of a straight regression line represent the void fraction ($\varepsilon = 0.47084 \pm 0.00355$) and the extra column volume ($V_{dead} = 0.28981 \pm 0.00614$ ml), respectively. The variances of these values are 95% confidence intervals. Comparing the value for V_{dead} extrapolated by this straight line with the experimental result using the connected adapters of the column ($V_{dead} = 0.31588 \pm 0.00459$ ml) indicates a slight overestimation of the extra column volume using connected adapters.

To distinguish band broadening introduced by the extra column space from the intra column broadening a plot of the total band broadening (σ^2_{total}) versus the retention volume (V_R) is shown (Fig. 2). The value of σ^2 at $V_R^2 = V_{dead}^2 = 0.083990$ of the regression line in Fig. 2 represents the lumped extra column broadening ($\sigma^2_{ex} = 0.01482 \pm 0.00122$ ml^2). This is caused by the application of the calculation of V_R^2 for $V_t = 0.0$ as shown in Fig. 1. The slope is the number of plates per unit length of the column ($1/N = 0.01470 \pm 0.00080$). The value of σ^2_{ex} extrapolated with the regression line is not significantly different from the value predicted from the experiment with connected adapters ($\sigma^2_{ex} = 0.01461 \pm 0.00175$ ml^2).

The data of these experiments also hint on the significant influence of the extra column broadening on the total broadening using very small columns. Therefore, a plot of the ratio of extra column broadening on the total broadening versus the column volume is shown (Fig. 3).

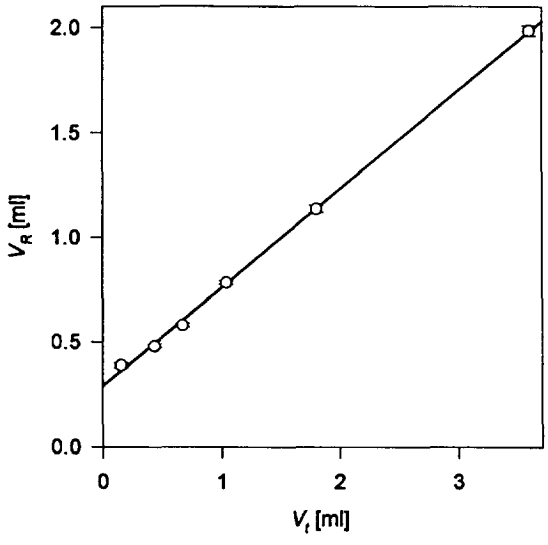

Fig. 1. Plot of retention volumes (V_R) against total column volumes (V_t) under non-binding conditions. Each data point with error bar represents a set of 15 experimental data points carried out at 5 different linear flow velocities (30.6, 76.4, 152.8, 305.6 and 611.2 cm/h). BSA pulse were applied on Q-HyperD, 50 m*M* Tris, 1 *M* NaCl, pH 8.0.

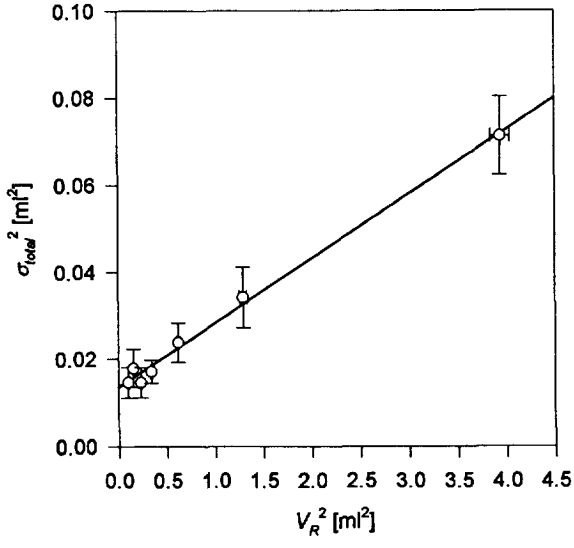

Fig. 2. Plot of total band broadening (σ^2_{total}) versus retention volume (V_R) under non-binding conditions. The regression line is according to Eq. (9). Each data point with error bars represents a set of 15 experimental data points at 5 different linear flow velocities (30.6, 76.4, 152.8, 305.6 and 611.2 cm/h). BSA pulse were applied on Q-HyperD, 50 m*M* Tris, 1 *M* NaCl, pH 8.0.

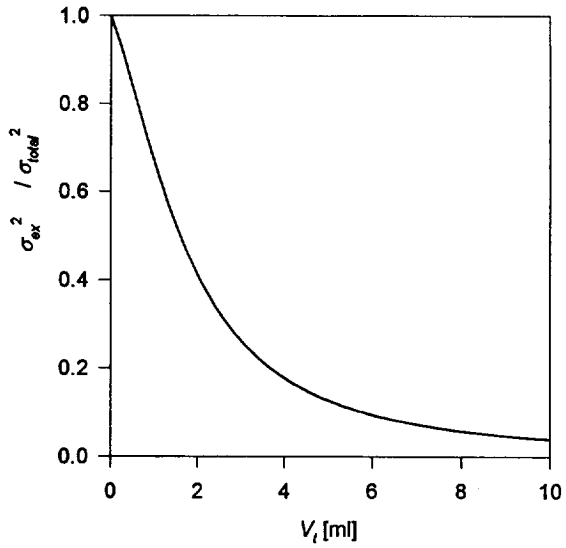

Fig. 3. Ratio of extra column broadening (σ^2_{ex}) on the total broadening (σ^2_{total}) versus the total column volume (V_t) calculated using the regression lines of Figs. 1 and 2.

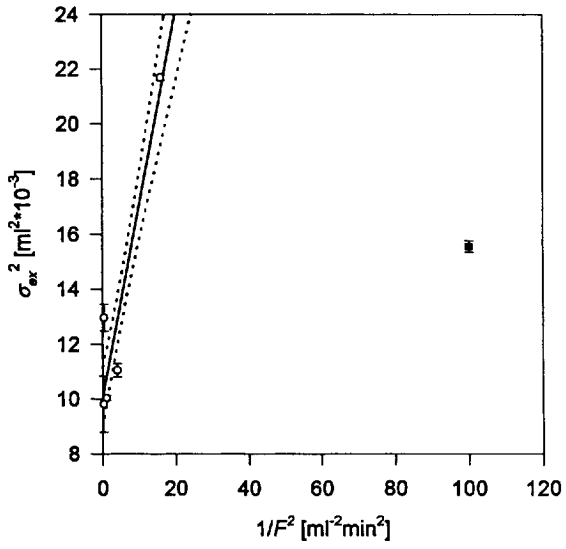

Fig. 4. Plot of extra column broadening variances versus inverse of the flow-rate and linear regression line with 95% confidence interval according to Eq. (6). Each data point with error bar represents 3 experimental data points obtained with two connected adapters. The data points symbolized by a gray square were excluded from the fitting procedure because of a significantly different peak shape at experiments with flow-rate 0.1 ml/min.

Fig. 3 indicates the big influence of the extra column broadening on the total broadening especially when using small columns. The extra column broadening of a column of a total column volume of 2 ml is about 40% and for a 1 ml column it is above 60%. For columns with 0.5 cm I.D. a total column volume of 1 ml is a normal case. For optimization of a chromatographic separation, experiments are carried out at the smallest possible scale. Therefore, a way to describe the extra column broadening was established.

Analyzing the peak variances of the experiments with connected adapters according to Eq. (5) indicates the contributions of the different types of broadenings on the extra column broadening. Fig. 4 shows the peak variances of experiments with connected adapters, that is no resin. The data points of experiments using 0.1 ml/min (30.6 cm/h) were excluded from the calculation of the regression line because of a significantly different peak shape compared to higher flow-rates (Fig. 5). The slope of

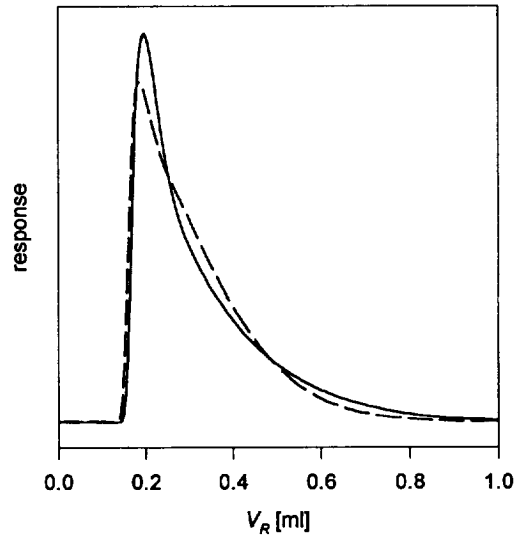

Fig. 5. Comparison of peak profiles of different flow-rates under non-binding conditions. BSA pulses were applied on a column with connected adaptors (V_t=0.0), 50 m*M* Tris, 1 *M* NaCl, pH 8.0. The solid line is a response curve at F=0.25 ml/min (u=76.4 cm/h). The peak shape is, as for all response curves at higher flow-rates, in good agreement with a exponentially modified Gaussian peak. The dashed line is a response curve at F=0.1 ml/min (u=30.6 cm/h). At this flow-rate the peak shape is completely different from the exponentially modified Gaussian shape.

the regression line in is equivalent to dispersion in the tubes ($\sigma_t^2 = 0.00304 \pm 0.00098$ ml^{3}min^{-1}) and the intercept to the sum of the variance of the initial sample profile and variances introduced by dead volumes ($\sigma_s^2 + \sigma_{dead}^2 = 0.00815 \pm 0.00203$ ml^2).

Comparing the values for σ_{total}^2 derived from this loading function with those derived from the regression shown in Fig. 4 indicates that they are in the same range. The corresponding values calculated using the regression line are 0.020289 ± 0.002625 ml^2 at $F = 0.25$ ml/min and 0.009668 ± 0.001674 ml^2 at $F = 2.0$ ml/min. Thus, there is no significant difference between these results. Analyzing the single contributions to the total broadening it can be seen that the Gaussian contribution is smaller than 5% of the total broadening.

This analysis also shows the dependency of variances of symmetrical Gaussian shape as well as variances of exponential decayed shape on the flow-rate. So, we can describe loading profiles for different sample volumes by changing the value of τ_r at different flow-rates by changing the values for σ and τ_e. In Fig. 6A the extrapolation to a 10 and 50 fold sample volume for a column of 5mm I.D. is shown. The response function of a pulse using a sample volume (V_S) of 0.02 ml was fitted by Eq. (16) and by altering the value of τ_r to $\tau_r = V_S = 0.2$ ml and τ_r to $\tau_r = V_S = 1.0$ ml the other profiles were described. While the extrapolation to $V_S = 0.2$ ml is in good agreement with the experimental data the extrapolation to $V_S = 1.0$ is not able to describe the strong tailing of the experimental profile. Fig. 6B gives a similar picture of a column of larger I.D. (26 mm).

Investigation of the dependencies of the fitting parameters σ, τ_e and V_R on the linear velocity u (Fig. 7) shows no strong correlation in the range of $u \geq 300$ cm/h. As this is the normal working range with the resin used, the influence of the flow-rate on the sampling function can be neglected.

The influence on the prediction of peak profiles using non-linear adsorption isotherms can be evaluated by applying the theoretically rectangular sample

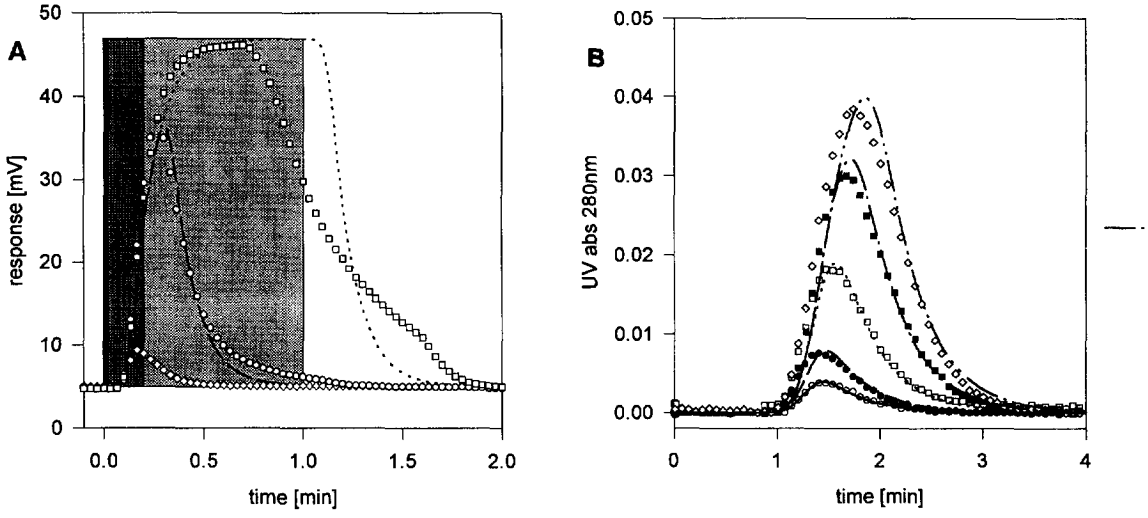

Fig. 6. Experimental and calculated peak profiles of different sample volumes. (A) Chromatographic system: FPLC as described in Section 3.1; Column I.D.: 5 mm, connected adaptors of a HR5 column. $F = 1.0$ ml/min ($u = 305.6$ cm/h). ◇ represents the experimental data at a sample volume (V_S) of 0.02 ml, these data were fitted according to Eq. (16) and used to extrapolate to higher sample volumes. ○ and ——— represent the experimental and calculated loading function at $V_S = 0.2$ ml, respectively; □ and · · · represent the experimental and calculated loading function at $V_S = 1.0$ ml, respectively. The rectangles represent the theoretical rectangular loading profile. The black rectangle represents $V_S = 0.02$ ml, the dark gray rectangle $V_S = 0.2$ ml and the light gray rectangle $V_S = 1.0$ ml. (B) Chromatographic system: ProSys as described in Section 3.1; Column I.D.: 26 mm, connected adaptors of a XK26 column. $F = 2.0$ ml ($u = 22.6$ cm/h). ○ represents the experimental data at $V_S = 0.1$ ml, these data were fitted (———) according to Eq. (16) and used to extrapolate to higher sample volumes. The extrapolated values are compared to the experimental values. $V_S = 0.2$ ml: ● experimental data and ——— extrapolated loading profile; $V_S = 0.5$ ml: □ experimental data and · · · extrapolated loading profile; $V_S = 0.954$ ml: ■ experimental data and – · – extrapolated loading profile; $V_S = 1.340$ ml: ◇ experimental data and – · · – extrapolated loading profile.

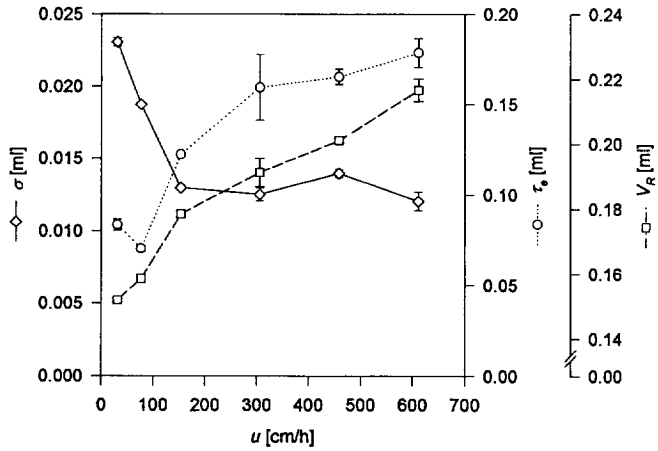

Fig. 7. Plot of fitting parameters σ, τ_e and V_R versus u. The solid line with diamonds indicates σ, the dotted line with circles indicates τ_e and the dashed line with squares indicates V_R. Each error bar represents three experimental values.

profile and the altered profile according to Eq. (16) to a peak prediction model. According to Fig. 8 there are different levels of complexity in taking extra column effects into account. The simplest way is to neglect all extra column alterations of the profile (Fig. 8A). Using Eq. (16) it is possible to take into account pre column extra column effects (Fig. 8B). The calculation of pre and post column extra column effects in a peak prediction program (Fig. 8C) is the most rigorous treatment and the only approach reflecting the real situation.

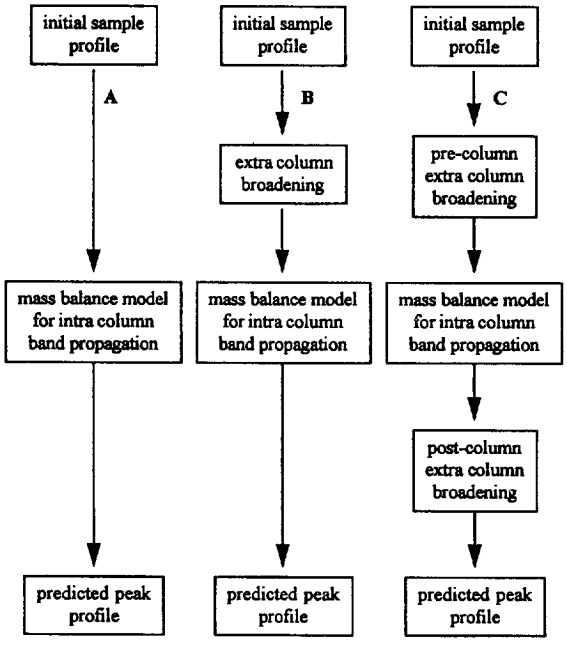

Fig. 8. Schematical drawing of the levels of complexity in the calulation of extra column effects. (A) extra column effects are neglected; (B) all extra column effects are taken into account pre column; (C) extra column effects are split into pre and post column effects.

Parameters for pre and post column broadening can be derived by fitting Eq. (28) to the experimental response profile. These parameters can be inserted into Eq. (16) to calculate pre and post column contribution independent from each other. The calculation according to Fig. 8C can be carried out by dividing the response profile of the mass balance model into rectangles of equal width. These numerous rectangles like an initial sample plug (Fig. 9).

Unfortunately, it is not possible to discriminate pre and post column extra-column broadening experimentally. Hence, there is no way to decide rationally if the fitted parameter τ_{e_1} or τ_{e_2} accounts for the pre column part of the system or vice versa. As a result, both opportunities must be calculated and only the comparison of predicted and experimental results can indicate the right choice (Fig. 10)

5. Discussion

Practical consequences lead to the use of small

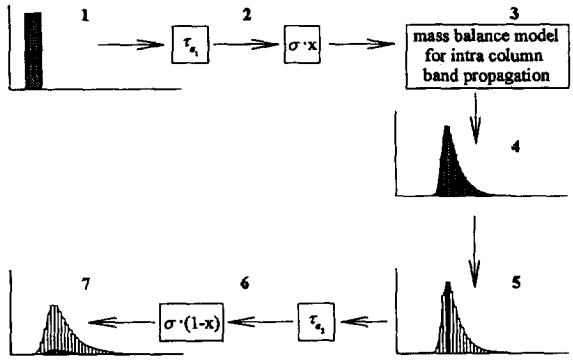

Fig. 9. Schematical drawing of the computation of a peak profile according to Fig. 8C. The initially rectangular sample profile (1) is altered pre column with an exponential decay function and a Gaussian broadening (2). This profile enters the mass balance model for intra column band propagation (3) and is broadened and retained according to the properties of the chromatographic column. The resulting response profile (4) is split up into rectangles (5). Each of the subsequent rectangles is altered post column with an exponential decay function and a Gaussian broadening (6). The final response profile (7) is built by summation of the individual profiles of the rectangles in (5). The grayed rectangles in (5) and (7) demonstrate this procedure. x in (2) and (6) represents the ratio between pre and post column extra column Gaussian broadening according to Eq. (25).

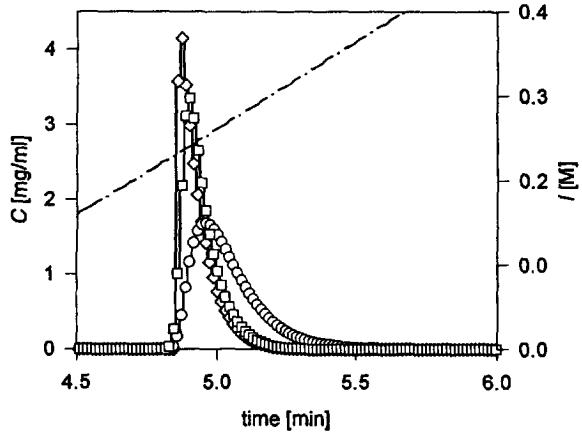

Fig. 10. Comparison of simulated peak profiles for linear gradient elution for the three different calculation schemes shown in Fig. 8. – ◇ – is the curve obtained when all extra column effects are assumed to be pre column (σ=0.022176 min, τ_e=0.101770 min); – □ – is the peak profile obtained when the major part of the extra column effects is assumed to be pre column (σ=0.022176 min, τ_{e1}=0.101256 min and τ_{e2} =0.008451 min); – ○ – is the peak profile obtained when the major part of the extra column effects is assumed to be post column. (σ=0.022176 min, τ_{e1}=0.008451 min and τ_{e2}=0.101256 min). In both of the latter calculations the Gaussian broadening is split in two equal parts for pre and post column broadening (x=0.5). – · – salt gradient. Simulation parameters: Freundlich isotherm with asymmetric logistic dose response (according to Kaltenbrunner and Jungbauer [18]): a= 241.063; b=0.766071; c=2.58254; d=122.096; e=0.0357043. Column: d=0.5 cm; L=5 cm; Np=32; Nps=40; ε=0.47. Gradient: I_0=0.01 M, I_{elu}=1.01 M, V_G=10 V_0, F=1.0 ml/min, Sample: C_0=20 mg/ml, V_S =0.02 ml.

columns in preparative chromatography. Band broadening can be measured easily by the second central peak moment. Electronic data acquisition in combination with the correct model for the chromatographic peak gives a very accurate measure for the peak width. A column with the identical connections to the chromatographic system has been used for the accurate experimental determination of the extra column effects. Therefore, this column has been packed with different amounts of chromatographic media. The only variable in the experimental set up is the column length. A protein pulse under non-binding conditions has been injected. Extra column space, void fraction, total broadening, extra column broadening and the number of plates per unit length of the column could be determined (Figs. 1 and 2). Putting the upper and lower adapter together yielded in the same range of extra column broadening as derived by using Eq. (9) to extrapolate to V_t=0.0ml. Fig. 3 demonstrates the relationship between V_t and the ratio between σ^2_{ex} and σ^2_{total}. The ratio of the calculated values σ^2_{ex} and σ^2_{total} (based on the regressions in Figs. 1 and 2) are plotted against V_t. Small columns as frequently used for optimization of preparative chromatography exhibit enormous σ^2_{ex}. For a 1 ml column approximately 60% of the total broadening is caused by extra column effects.

Preliminary results from experiments with varying flow-rates (F) show that band broadening can be described by Eq. (6) within a certain range of F (Fig. 4). Comparing the peaks attained at a very low flow-rate and a high flow-rate using only connected adapters, a significantly different peak shape can be observed (Fig. 5).

The extra column band broadening with respect to sample volume has been modeled by convolution of the Laplace transforms of a rectangular plug of the width of the sample volume and an exponential decay and a Gaussian contribution to broadening Eq.

(16). For a certain sample volume the broadening can be predicted by this model using the parameters from one experiment. These parameters are easily accessible by fitting Eq. (16) to the response peak. Inserting these parameters into Eq. (16), the broadening for different initial pulse widths can be predicted (Fig. 6A and B).

Fig. 7 shows the relationship between σ, τ and the flow-rate. Above 300 cm/h, the working range of novel chromatographic media, minor influence from the flow-rate can be expected. Fig. 7 is consistent with the findings described above (Figs. 4 and 5).

The crucial point in our concept is the experimental determination of pre and post column contribution to broadening. A theoretical access to this problem is possible by simulation. Varying the ratio between pre and post column contribution for σ and τ provides an insight. Introduction of pre and post column band broadening increases the complexity but provides fundamental information on the design of the experiment, since the major contributions to band broadening are revealed. This simulation will be also very useful for scale up and scale down studies. The parameters for calculation of extra column effects can be determined at different scales, which subsequently will allow calculations of band broadening at different scales. Transfer to another scale will not be an empirical operation any longer.

6. Symbols

6.1. Latin symbols

D_M	molecular diffusion coefficient
F	volumetric flow-rate
h	increment of numerical approximation in length domain
HETP	height equivalent to a theoretical plate
k_0'	retention factor
L	column length
N	number of theoretical plates
r	radius of tube or column
s	Laplace operator
$T_1,\ldots T_8$	subterms of Eqs. (16) and (28)
u	linear velocity of mobile phase
V_d	sensitive detector volume
V_{dead}	dead volume
V_S	sample volume
V_t	total column volume

6.2. Greek symbols

ε	void fraction
Λ	unit step function f(t) $=0$ for $t < \tau_r$ and f(t) $=1$ for $t > \tau_r$
σ_A^2	variances independent of the flow-rate
σ_B^2	variances dependent on the flow-rate
$\sigma_{c.i.}^2$	intra column broadening
σ_d^2	contribution of sensitive detector volume to band broadening
σ_{ex}^2	lumped extra column dispersion
σ_{pre}^2	pre column Gaussian broadening
σ_{post}^2	post column Gaussian broadening
σ_s^2	variance of the initial theoretical injection profile
σ_t^2	variance introduced by dispersion in tubes
σ_{total}^2	total band broadening
τ	increment of numerical approximation in time domain
τ_{dead}	contribution of dead volume to band broadening
τ_e	exponential time constant of an exponential decay function
τ_{e1}	pre column exponential broadening
τ_{e2}	post column exponential broadening
τ_{el}	contribution of finite response rate of electronics to band broadening
τ_r	width of a rectangular sample plug

References

[1] J.C. Sternberg, Adv. Chromatogr., (1966) 205.
[2] J.F.K. Huber and A. Rizzi, J. Chromatogr., 384 (1987) 337.
[3] E.V. Dose and G. Guiochon, Anal. Chem., 62 (1990) 1723.
[4] J.Å. Jönsson, in J.Å. Jönsson (Editor) Chromatographic Theory and Basic Principles, Marcel Dekker, New York, 1987, Ch. 2, p. 27.
[5] J.L. Rocca, J.W. Higgins and R.G. Brownlee, J. Chromatogr. Sci., 23 (1985) 106.
[6] Q.M. Mao, I.G. Prince and M.T.W. Hearn, J. Chromatogr. A, 691 (1995) 273.
[7] Q. Yu and N.-H. L. Wang, Comput. Chem. Eng., 13 (1989) 915.
[8] S. Golshan-Shirazi and G. Guiochon, J. Chromatogr. A, 658 (1994) 149.

[9] S.R. Gallant, A. Kundu and S.M. Cramer, J. Chromatogr. A, 702 (1995) 125.
[10] A. Jungbauer and O. Kaltenbrunner, Biotechnol. Bioeng., 52 (1996) 223–236.
[11] G. Taylor, Proc. Roy. Soc. London, Ser. A, 219 (1953) 186.
[12] S.P. Cram and T.H. Glenn, J. Chromatogr., 112 (1975) 329.
[13] H. Poppe, Anal. Chim. Acta, 114 (1980) 59.
[14] E. Grushka, Anal. Chem., 44 (1972) 1733.
[15] P. Naor and R. Shinnar, I&EC Fund., 2 (1963) 278.
[16] J.P. Foley and J.G. Dorsey, Anal. Chem., 55 (1983) 730.
[17] M. Abromovitz and I.A. Stegun, Handbook of Mathematical Functions, Dover, New York, 1965.
[18] O. Kaltenbrunner and A. Jungbauer, J. Chromatogr. A, 734 (1996) 183.